

Evolution enhances mutational robustness and suppresses the emergence of a new phenotype

Tadamune Kaneko^{1,2} and Macoto Kikuchi^{2,1*}

¹ *Department of Physics, Osaka University, Toyonaka 560-0043, Osaka, Japan*

² *Cybermedia Center, Osaka University, Toyonaka 560-0043, Osaka, Japan*

Gene regulatory networks (GRN) have developed their functions through evolution, thus reflecting the evolutionary histories they followed. Some of their properties could be consequences of the particularity in the evolutionary mechanism, and some may be more universal, determined largely by external conditions. To understand the universality and particularity of the evolutionary process theoretically, evolutionary simulations (ES) alone are insufficient, because the outcomes of ES depend on evolutionary pathways. Thus, a reference system is required. The appropriate reference system for this purpose is a set of randomly sampled GRNs. In this study, we constructed a reference set using the method proposed by Nagata and Kikuchi (PLoS Comput Biol 16 (2020) e1007969) and compared it with the results of ES. While this approach can be applied to evolution in general, we focused on the emergence of bistability and enhancement of mutational robustness by evolution. We found the following results: First, random sampling revealed that GRNs with high fitness exhibited bistability when we required a sensitive response to environmental change. The increase in the fractions of bistable GRNs in ES occurred at higher fitness levels than those in the reference set. Therefore, the emergence of a new phenotype, bistability, was delayed in evolution. Second, mutational robustness was significantly higher in ES than in the reference set. Therefore, the mutational robustness was enhanced by evolution. Bistable GRNs contain many mutationally fragile GRNs compared to non-bistable GRNs. This implies that the delayed emergence of bistability is a consequence of the mutation-selection mechanism of evolution. Third, evolution begins to slow down significantly at the fitness level where the number of available GRNs begins to decrease rapidly. This implies that evolutionary speed is determined mainly by “genotypic entropy.”

I. INTRODUCTION

Since living systems have developed through the long history of evolution, their present forms reflect the evolutionary histories they followed. If we regard evolution as a kind of optimization process, although this view is too simplified, it is natural to expect that the evolution process comprises some features that are different from those of other optimization processes. Thus, some properties of living systems should be consequences of such a particularity of evolution. In contrast, some properties may be more universal so they do not depend on the evolutionary process. Such universal properties may be largely constrained by environmental conditions. In this respect, the universal properties and particularities of evolution are of interest. However, experimental studies on this topic are limited because existing living organisms are products of evolution; thus, evolutionary experiments can only provide outcomes reflecting evolutionary histories. Therefore, numerical methods play an indispensable role in obtaining information on the universality and characteristics of evolution.

Although evolutionary simulation (ES) is a powerful method for studying the evolution process numerically, its outcomes depend strongly on the evolutionary pathways; therefore, ES alone is insufficient for our purpose. We require a reference system for comparison. In this

study, we investigated the evolution of gene regulatory networks (GRNs). A reference system that could be considered natural for this case is a set of all possible GRNs. However, enumeration of all the networks is impossible unless we restrict ourselves to very small GRNs. Thus, the reference system we consider appropriate is a set of randomly sampled GRNs. If some properties are universally observed in that set, they should be realized universally irrespective of the evolutionary pathway. If there are some differences between the results of ES and the reference set, they are manifestations of the particularity of evolution. We propose a research method for determining the properties of the evolutionary process by comparing a randomly sampled set of GRNs obtained using a method based on statistical mechanics with the GRNs obtained using ES. While this method can be applied to studies of evolution in general, we focused on the emergence of bistability and evolution of mutational robustness.

Living systems have not only adapted to the environment through evolution but have also acquired many types of robustness, such as robustness against environmental and internal noises as well as that against genome mutations[1–3]. Among the various types of robustness, the most important is mutational robustness, which enables a living system to not lose its function and continue to exist even when its genome is mutated.

Mutational robustness has been demonstrated experimentally. For example, comprehensive single-gene knockout experiments for bacteria and yeasts have revealed that most gene knockouts do not affect viability[4–6].

*kikuchi@cmc.osaka-u.ac.jp

An artificial rewiring experiment for the GRN of *E. Coli* showed that the bacterium remains viable after most artificial additions of regulatory links[7]. Since living systems are constantly subjected to genetic mutation, if they easily lose their functions, they will not produce offspring during the evolutionary process. Therefore, mutational robustness must be enhanced through the evolutionary process along with the functions of living organisms. Mutationally robust genotypes have been selected because of the mutation-selection mechanism of evolution, and this selection is not directly related to any function. Thus, the enhancement of mutational robustness through evolution is called "second-order selection"[2].

To determine whether mutational robustness is enhanced by evolution, we required randomly sampled GRNs as a reference system independent of evolutionary pathways, as stated above. Random sampling is suitable for identifying universal properties that do not depend on the history of evolution. Ciliberti *et al.* conducted a random sampling of GRNs to investigate mutational robustness[11, 12]. The fitness of their model had only two values – viable and non-viable. They investigated the interrelations of viable GRNs and argued that majority of GRNs belong to a large cluster connected by neutral mutations, similar to the neutral networks found in the RNA sequence space[13]. However, such a simple random sampling method is not useful for systems with a more complex fitness landscape, because highly fit GRNs are rare. Burda *et al.* and Zagorski *et al.* employed the Markov chain Monte Carlo method to sample highly fit GRNs[14, 15]. They found that GRNs exhibiting multistability contained a common network motif. These studies focused on the universal properties of highly fit GRNs.

The abovementioned methods are insufficient for sampling GRNs with a wide range of fitness levels. Saito and Kikuchi proposed the use of the multicanonical Monte Carlo (McMC) method to investigate the mutational robustness of GRNs[16]. McMC was originally developed in the field of statistical physics for sampling configurations within a wide range of energies[17, 18]. However, this method has also been found to be useful for sampling nonphysical systems. It is particularly effective for generating very rare states and estimating the appearance probabilities of such rare states[19–23].

Using McMC, Nagata and Kikuchi investigated a GRN model[24]. They regarded fitness as the "energy" of GRNs and sampled GRNs with very low fitness to very high fitness, and then classified the GRNs by fitness to explore the universal properties that are independent of evolutionary pathways. They considered a neural network-like model of GRN, with one input gene and one output gene, and set the fitness such that it was high if the GRN responded sensitively to changes in the input. As each gene in their model did not respond ultrasensitively[25, 26], and the network structures were restricted, simple network motifs did not give rise to bistability[27]. Despite this, they found that highly fit

GRNs always exhibited bistability. Therefore, bistability emerges as a consequence of the cooperation of many genes. According to their results, a new phenotype of bistability appears, regardless of the evolutionary path a system follows. In addition, they found that mutationally robust GRNs were not rare among highly fit GRNs.

Bistable or multistable responses of GRNs are widely observed in living systems. The best-known example is the toggle switch for lysogenic-lytic transition in phage λ , which has been extensively studied both experimentally and theoretically [28–31]. Another example is the *cdk1* activation system of *Xenopus* eggs [32–34]. The bistable switches of GRNs are also utilized in cell-fate decisions; a well-known example is the bistability of the MAPK cascade which regulates the maturation of the *Xenopus* oocyte[35]. While the roles of small motifs have been the focus of such systems, the importance of cooperativity of many genes has been stressed theoretically[36]

In this study, we extended the research of Ref. [24] to more general network structures and investigated the characteristics of evolution. By comparing the results of McMC and ES, we explored the enhancement of the mutational robustness by evolution and how evolution affects the emergence of bistability.

II. MODEL

Genes coded by DNA in cells are read by RNA polymerase and transcribed to mRNA, the information in which is then used to assemble proteins. A category of proteins called transcription factors act as activators or repressors of other genes. Many genes regulate each other in this way and form a complex network called a GRN. GRNs are used to change the cell state to adapt to environmental changes or to control the cell cycle or cell differentiation. One of the best-known GRN mathematical models is the Boolean network model proposed by Kauffman, in which each fixed point of the dynamical system is considered to represent a cell state[8–10].

In this study, we considered regulatory relations and ignored the details of gene expression. Such connectionist-type modeling has been widely used in theoretical studies[24, 36–44]. We represented GRNs as directed graphs, with nodes as genes and edges as regulatory interactions. For simplicity, we consider GRNs with one input node and one output node. In contrast to Ref. [24], wherein several restrictions were imposed on the network structure, we allowed any network as long as the number of edges from one node to another was at most one. Therefore, GRNs could contain auto-regulation and mutual regulation. Nodes and edges that did not contribute to the output were also permitted. As a result, the effective network size could be smaller than the prepared size. In the following sections, we have restricted the discussion to networks with $N = 32$ nodes and $K = 80$ edges.

A variable $x_i \in [0, 1]$ that represents the expression

of a gene is assigned to each node, where i indicates the node number. x_i obeys the following discrete-time dynamics[38, 39]:

$$x_i(t+1) = R\left(I\delta_{i,0} + \sum_j J_{ij}x_j(t)\right), \quad (1)$$

where t denotes the time step. J_{ij} represents the regulation from the j -th node to the i -th node. For simplicity, we assume that J_{ij} takes one of the three values $-0, \pm 1$; $+1$ indicates activation, -1 indicates repression, and 0 indicates the absence of regulation. The 0th node was the input gene, and $I \in [0, 1]$ was the strength of the input signal[44]. The response of the genes was given by the following sigmoidal function:

$$R(x) = \frac{1}{1 + e^{-\beta(x-\mu)}}, \quad (2)$$

where β represents the steepness of the function, and μ is the threshold. This function is widely used in theoretical studies[36, 40, 44–46]. In the present study, we set $\beta = 2$ and $\mu = 0$. These parameters are the same as those for the neural network model used by Hopfield and Tank[47] and provide a gradual increase to the response function, which reflects the stochastic nature of gene expression[36]. The response function $R(x)$ with $\mu = 0$ is not ultrasensitive because a single gene with this response function has a single fixed point even when the auto-activation loop is attached. Therefore, for the emergence of multistability, many genes must act cooperatively. An example of the parameters of $R(x)$ that a single gene with an auto-activation loop exhibits bistability is $\beta = 6$ and $\mu = 0.5$. Although the spontaneous expression $R(0) = 0.5$ is rather large, we do not believe that it caused any problems in the present investigation.

Following the definition of the fitness presented by Ref. [24], we set the fitness so that it was larger when the difference in the expression levels of the output gene between $I = 0$ and 1 (“off” and “on”) was large. $\bar{x}_{out}(I)$ was the fixed-point value of the output node for fixed I ; as the initial condition, we set the expression of all genes as 0.5 , the spontaneous expression. If $x_{out}(t)$ behaved oscillatorily over time instead of reaching the fixed point, we used the temporal average for $\bar{x}_{out}(I)$; in most cases, the system reached a fixed point. Fitness f was defined as follows:

$$f = |\bar{x}_{out}(0) - \bar{x}_{out}(1)|. \quad (3)$$

Fitness takes a value in $[0, 1]$ by definition.

We sampled GRNs using MCMC (hereafter, “random sampling”) and ES. For each ES, we prepared a random population consisting of thousand GRNs. Two types of ES were made: in one type, half of the GRNs in the population were preserved at each generation, and in another type, 90% of GRNs were preserved. We refer to them as Evo50 and Evo90, respectively. In the following sections, we mainly show the results of Evo50, unless otherwise stated. Details of the computational methods are summarized in the Method section.

III. RESULTS

A. Fitness landscape and speed of evolution

The blue line in Fig 1(a) shows the base 10 logarithm of the appearance probability $\Omega(f)$ for each bin of fitness f obtained by random sampling. This is referred to as the fitness landscape. The sum of $\Omega(f)$ was normalized to 1. The probability for $f \geq 0.99$ was $\sim 10^{-16}$. Because we can count the total possible number of GRNs as $\binom{N^2}{K}2^K \simeq 10^{145}$, highly fit GRNs are numerous but rare. The fitness landscape is divided roughly into three regions. The majority of GRNs concentrate near $f \sim 0$. Then, the number of GRNs decrease exponentially with f , and, for a very high f , they decrease faster than the exponential rate. For comparison, we have shown the fitness landscape for a steeper response function, $\beta = 4$ and $\mu = 0$, in Fig 1(b). Although the fitness landscape is jaggy (it is not due to statistical error), it also consists of three regions, namely, the majority around $f \sim 0$, the exponential decrease, and the faster-than exponential decrease, as in the case of $\beta = 2$.

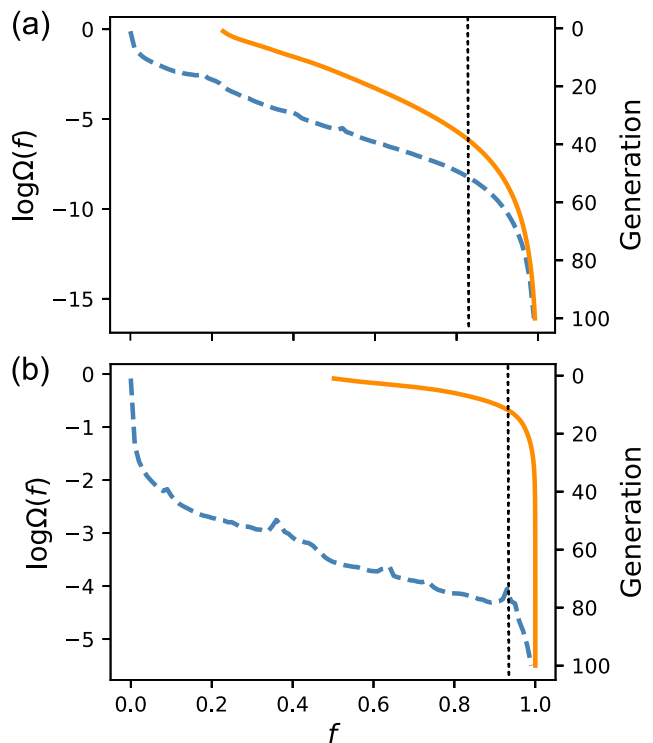


Fig 1: **Fitness landscape and evolution of fitness.** The fitness f is divided into 100 bins. The blue dashed lines (left axis) show the base 10 logarithm of the appearance probability $\Omega(f)$ of each bin, which was obtained by random sampling. The orange solid lines (right axis) represent the average fitness of each generation calculated for lineages obtained by Evo50. Averages were taken over 100,000 lineages. The vertical lines indicate the fitness at which $\Omega(f)$ starts to decrease faster than the exponential rate. (a) $\beta = 2$ and $\mu = 0$. (b) $\beta = 4$ and $\mu = 0$.

The orange lines represent the average fitness of each generation obtained by Evo50. The vertical axis represents the generation in the downward direction. The evolution progresses almost linearly in the early stage and slows down drastically for a large f . The values of f for which the increase in fitness starts to slow down roughly coincides with the values for which the faster-than-exponential decrease in $\Omega(f)$ begins for both $\beta = 2$ and 4. This may be because the number of possible destinations that a GRN can transit to by the mutation is restricted by $\Omega(f)$. In other words, when the number of GRNs with higher fitness levels decreases drastically, the possibility that the fitness increases by chance also decreases. A comparison of Evo50 and Evo90 for $\beta = 2$ is given in S1 Fig. Although the evolution was slower for Evo90, the overall tendency was similar. Since $\log \Omega(f)$ can be called “genotypic entropy”, this result suggests that evolutionary speed depends in a large part on genotypic entropy.

B. Delayed emergence of bistability

The model in Ref. [24] exhibits bistability as f approaches its maximum value. In other words, the dynamical system reaches different fixed points for $I = 0$ and 1. When I is changed continuously, two saddle-node bifurcations occur, in contrast to the case of a small f , wherein a single fixed point moves to follow the change in I . We call the latter type of GRNs monostable. We found that the present model behaves similarly despite the fact that the network structures are largely different owing to different restrictions imposed on the network construction.

Bistable GRNs are classified into three categories. The first is the toggle switch, in which two saddle-node bifurcations occur within $I \in [0, 1]$. The toggle switch is found, for instance, in phage λ and utilized for adaptation to environmental change[28–30]. The second is the one-way switch[48]. In this case, only one saddle-node bifurcation point is found in the range $I \in [0, 1]$, and another bifurcation point is present outside this range. One-way switches give rise to cell maturation or cell differentiation; a typical example of such switches is the MAPK cascade in the maturation of *Xenopus* oocytes[35]. In the last category, both bifurcation points were outside the range of I . Since this type may not work as a switch as long as the effect of noise is not taken into account, we called it “unswitchable.” In this study, we do not distinguish these three and treat them equally as bistable GRNs. It is straightforward to change the definition of bistability to deal only with, for example, toggle switches.

First, we investigated bistability using a strict criterion. Bistability was checked as follows: Starting from the steady state at $I = 0$, I was increased by 0.001, and the dynamics were run until the steady state was reached. This procedure was repeated for up to $I = 1$. Then, the inverse process, from $I = 1$ to 0, was performed. If a

difference in \bar{x}_{out} larger than 10^{-6} was observed between these two processes in a range of I , the GRN was regarded as bistable. We employed such a strict criterion because the monostable GRNs and the bistable GRNs were intrinsically different dynamical systems. We may regard the emergence of bistability as the emergence of a new phenotype.

Fig 2(a) shows the fraction of bistable GRNs $P_2(f)$ against fitness. The blue line is the result of random sampling. The bistable GRNs began to appear at $f \simeq 0.5$ and increased rapidly until all GRNs became bistable for $f \rightarrow 1$. Therefore, the new phenotype of bistability emerged as the fitness increased, and all GRNs converged to such a phenotype as the fitness approached its maximum value. The orange and green lines are the results of Evo50 and Evo90, respectively. For all the data, the standard errors were smaller than the mark. We classified GRNs in the obtained lineages by fitness, as with random sampling. Fig 2 (a) shows that $P_2(f)$ of ES was substantially low compared to that of random sampling at the same f . In other words, evolution delays the rapid increase of $P_2(f)$. This suggests that evolution tends to suppress the emergence of a new phenotype; nonetheless, the eventual emergence of the bistable phenotype is inevitable as the fitness increases, because all GRNs are bistable for $f \rightarrow 1$. Evo50 and Evo90 behave similarly except for the early stage of increase; Evo90 initially coincides with the random sampling and soon confluent with Evo50. This indicates that the emergence of bistability in evolution depends, in part, on evolutionary speed.

Although the strict criterion of bistability employed above is mathematically meaningful, very weak bistability may be biologically irrelevant, because it may not be distinguishable from monostability in living systems. Thus, we also investigated the bistability using a looser criterion; the checking interval of I was set at 0.01 and the criterion of bistability was set as a difference in \bar{x}_{out} larger than 0.5. The results are shown in Fig 2(b). While the rapid increase in the bistable GRNs moves to a higher f than (a), the tendency that the emergence of bistability is delayed in evolution compared to that of random sampling is unchanged. Therefore, we consider that the delayed emergence of bistability is a biologically relevant phenomenon.

C. Evolutionary enhancement of mutational robustness

To discuss mutational robustness, we introduced a measure of robustness. In Ref. [24], a single-edge deletion was considered as a mutation; it was found that the edges split into two classes, neutral and lethal, for highly fit GRNs, and the lethal edges were minor among them. We considered a single-edge deletion as a mutation also for the present model and obtained similar results. Then, we defined the following quantity r as the robust-

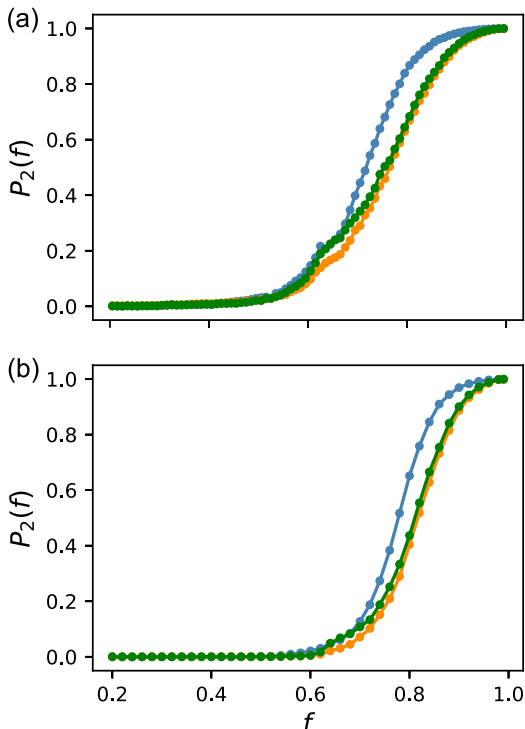


Fig 2: **Fitness dependence of the fraction of bistable GRNs.** The blue line represents the random sampling. The orange and green lines represent Evo50 and Evo90, respectively. The standard errors are smaller than the mark. Bistability was checked as follows. First, starting from the steady state at $I = 0$, I increased by ΔI , and the dynamics were run until the steady state was reached. This procedure was repeated for up to $I = 1$. Then, the inverse process, from $I = 1$ to 0, was performed. If a difference in \bar{x}_{out} larger than the threshold x_{th} was observed between these two processes in a range of I , the GRN was regarded as bistable. GRNs obtained by ES were classified according to f into 100 bins, similar to random sampling. (a) Strict criterion, $\Delta I = 0.001$ and $x_{th} = 10^{-6}$. (b) Loose criterion, $\Delta I = 0.01$ and $x_{th} = 0.5$.

ness measure:

$$r \equiv \frac{1}{K} \sum_{i=1}^K f'_i, \quad (4)$$

where f'_i is the fitness after the i th edge is deleted, and the sum is taken for all edges. Because r should increase with f , comparing r of GRNs with different f is not meaningful. However, by comparing this quantity for GRNs obtained by random sampling and ES at the same f , we can investigate how evolution affects mutational robustness.

Fig 3 shows the average of r against f for the random sampling, Evo50, and Evo90. The average was taken over all the GRNs in the corresponding bin. For the highest fitness of the ES, only the data in the range $[0.990, 0.991)$ were used. $\langle r \rangle$ obtained by ES increased monotonically and coincided with those obtained by random sampling up to $f \simeq 0.5$. For larger f , the value of evolution de-

parted upward from that of random sampling, and the difference became increasingly significant as f increased. Evo50 and Evo90 behave almost similarly, except for the highest fitness, where Evo90 exhibits a slight decrease. The reason for this decrease is not clear, but the standard errors are very small, and this decrease is not due to a statistical error.

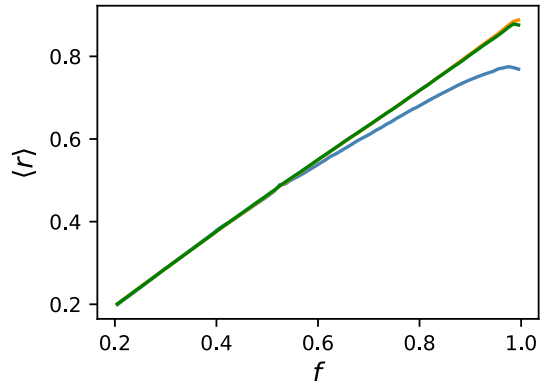


Fig 3: **Average of the robustness measure r against fitness.** The average was taken over all the samples in each bin. The blue line represents random sampling. The orange and green lines represent Evo50 and Evo90, respectively. The slight decrease at the highest fitness for Evo90 was not due to a statistical error.

To scrutinize the difference, we show the probability distributions of r for $f \in [0.5, 0.51)$, $[0.8, 0.81)$, and $[0.99, 1.0]$ in Figs. 4(a)-(c), respectively. The data for ES are taken from Evo50. Considering that the distribution of f within each bin differs for random sampling and ES, we divided each bin into ten sub-bins and reweighed the distribution obtained by ES, so that the distribution of f coincided with that of random sampling. While both distributions roughly agreed for $f \in [0.5, 0.51)$, we observed a deviation for $f \in [0.8, 0.81)$. The two distributions exhibited distinct differences for $f \geq 0.99$, and the distribution obtained by ES was biased to a large r compared to random sampling. Therefore, it was shown that evolution enhanced the mutational robustness.

What caused this difference in the distributions? As stated previously, the edges of randomly sampled GRNs for $f \geq 0.99$ are split into two classes: neutral and lethal. That is, when we delete one edge, f' is either close to f or almost zero, and other types of edges are scarce. Therefore, we investigated the number distribution of the lethal edges for $f \geq 0.99$ by stating that an edge is lethal if $f' < 0.8$. Although this definition is arbitrary, it hardly affects the results. Fig 5 shows the probability distribution of the number of lethal edges n_L . GRNs obtained by ES are significantly biased toward a small number side compared to random sampling. The highest probability was at $n_L = 3$, and the distribution was narrow; moreover, more than 2% of GRNs had no lethal edge. In contrast, the highest probability for random sampling was at $n_L = 15$, and the distribution was much

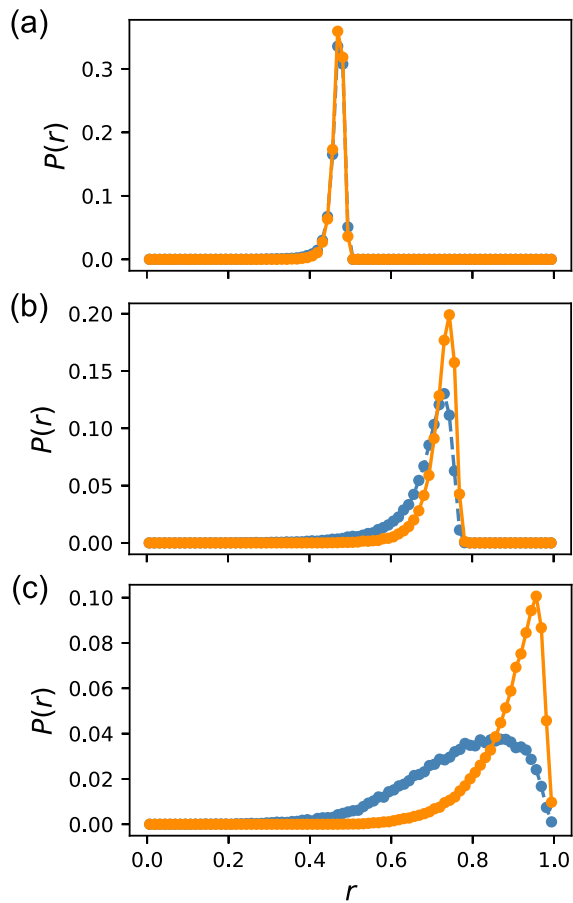


Fig 4: **Probability distributions of the robustness measure r .** (a) $f \in [0.5, 0.51]$ (b) $f \in [0.8, 0.81]$ (c) $f \in [0.99, 1.0]$. The orange solid lines represent Evo50 and the blue dashed lines represent random sampling. r was divided into 80 bins because, otherwise, unnecessary oscillation appeared in the distribution, owing to the discreteness of the number of lethal edges. The distributions for ES were corrected using the reweighting method described in the text.

broader. The number of GRNs lacking a lethal edge was only 0.4%. Therefore, the small number of lethal edges is the cause of the enhancement of mutational robustness by evolution.

One possible explanation for this is that the nodes that affect the output are fewer in the evolutionarily obtained GRNs. To check this, we counted the number of nodes n_N that had at least one path to the output node. Fig 6 shows the distributions, and the distribution of the random networks is also plotted for comparison. While the peak of the distribution was at $n_N = 28$, which is slightly less than that for the peak of random networks, the distributions were indistinguishable between ES and random sampling. Therefore, the number of effective nodes is not the cause of the difference in the number of lethal edges.

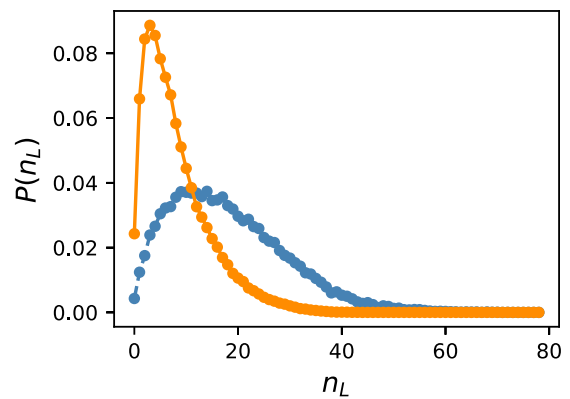


Fig 5: **Probability distribution of the number of lethal edges n_L .** The data for $f \in [0.99, 1.0]$ are shown. An edge is regarded as lethal if the fitness f' becomes less than 0.8 after the edge is deleted. The orange solid line represents Evo50, and the blue dashed line represents random sampling. The distribution for ES was corrected using the reweighting method described in the text.

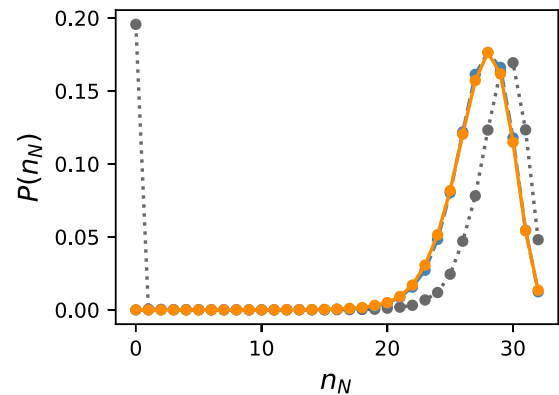


Fig 6: **Distribution of the number of effective nodes n_N .** The data for $f \in [0.99, 1.0]$ are shown. If a node has at least one path to the output node, the node is regarded as “effective”. The orange solid line represents Evo50, the blue dashed line represents random sampling, and the grey dotted line represents random networks as a reference. The distribution for ES was corrected using the reweighting method described in the text.

D. Motif analysis

Next, we investigated the network motifs. In the model presented in Ref. [24], coherent feedforward loops (FFL+), and positive feedback loops (FBL+) were significantly abundant in highly fit GRNs. Since the present model allows both auto- and mutual-regulations, we also explored other patterns than the triangular patterns. We counted the number of auto-regulations, mutual-regulations between node pairs, triangles, and mutual-activation or mutual-repression of two nodes accompanied by auto-activations of both nodes. Because the motifs are defined as network patterns that are abundant compared to random networks[27, 49], we also counted

them for random networks.

As a result, the following patterns were greater in number than the random networks: auto-activation, mutual-activation, mutual-repression, FFL+, FBL+, mutual-activation accompanied by auto-activations of both nodes, and mutual-repression accompanied by auto-activations of both nodes. Although their abundances were not remarkable, we called them motifs. The number distribution of auto-activation is shown in Fig. 7 (a), and that of the other motifs in S1 Fig. Other patterns, such as auto-repression, incoherent feedforward loop, and negative feedback loop, were fewer in number than random networks. In Fig. 7, we compare the number distributions of auto-activation and auto-repression; the former is a motif, while the latter is not. It should be noted that the number of auto-regulations is low. However, there are very few GRNs that do not undergo auto-activation. In contrast, almost half of the GRNs do not have auto-repression. Thus, auto-activation is favored compared to auto-repression.

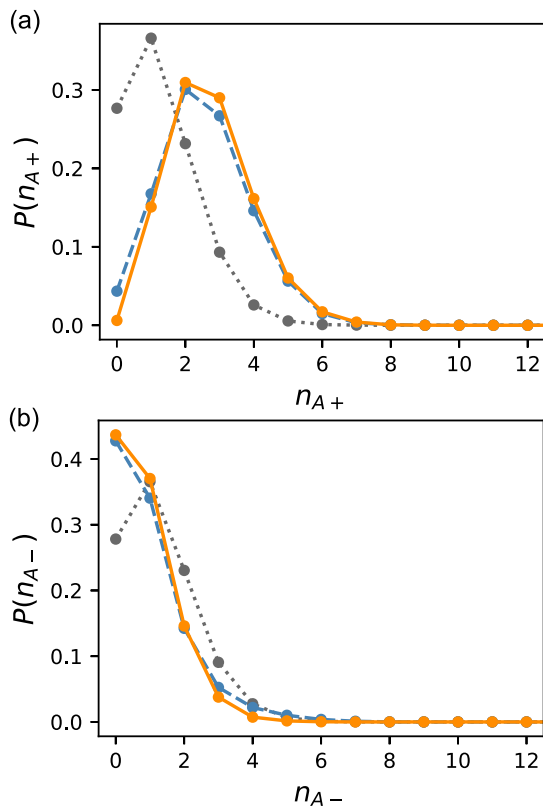


Fig 7: **Probability distribution of number of auto-regulations.** (a) Number of auto-activations n_{A+} . (b) Number of auto-repressions n_{A-} . The data for $f \in [0.99, 1.0]$ are shown. Orange indicates ES and blue indicates random sampling. The black dotted line represents the random networks as a reference. The distribution for ES was corrected using the reweighting method described in the text. Auto-activation is a motif, whereas auto-repression is not a motif.

Overall, the distributions of these motifs were almost

the same for both ES and random sampling. Therefore, whether these highly fit GRNs are products of evolution is not reflected in the distributions of these local motifs. This implies that the difference between evolution and random sampling should lie in global network structures.

E. Path distribution

As a characteristic of the global structure, we counted the number of paths n_{path} connecting the input and output nodes. Fig 8 (a) shows the distribution of paths starting from the input node and reaching the output node without passing the same node more than once. Two distributions exhibited a distinct difference; while the probability of GRNs with only one path reaches 4% for random sampling, it is 0.1% for ES. In addition, evolutionarily obtained GRNs with less than approximately 100 paths were fewer than GRNs obtained through random sampling. This suggests that the global structures of the GRNs obtained using these two methods differ significantly. However, the difference in path distribution does not explain everything. Fig 8 (b) is a scatter plot of the number of paths and the number of lethal edges. We took the data for $f \in [0.99, 0.991]$ from the evolutionarily obtained GRNs. The figure shows that the number of lethal edges is less for ES, irrespective of the number of paths. Even for $n_{path} = 1$, the number of lethal edges is distributed broadly. This means that the locations of the lethal edges were not limited to the “on-path” locations between the input and output nodes.

F. Relation between bistability and mutational robustness

So far, we have observed the enhancement of mutational robustness and the delayed emergence of bistability by evolution. Thus, we expected that there would be a relationship between them. Fig. 9 is a scatter plot of fitness f and robustness r for GRNs obtained by random sampling. Each point indicates a GRN. The orange points are for the monostable GRNs, and the blue points represent the bistable GRNs. These differences are pronounced. For monostable GRNs, r increases with f and is distributed within a narrow range. In contrast, bistable GRNs include those with very low robustness, irrespective of their fitness value. As a result, the robustness of bistable GRNs spreads widely. This difference implies that if relatively robust GRNs for mutation are favored by evolution, bistable GRNs would tend to be avoided.

G. Steady-state evolution of the mutational robustness

Evolutionary simulations would eventually reach the steady state, and the robustness distribution in the

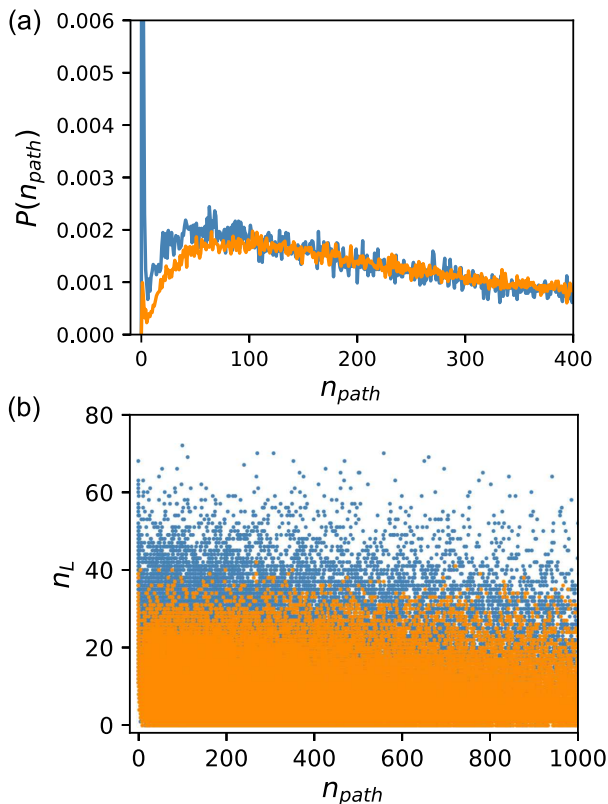


Fig 8: **Number of paths n_{path} starting from the input node and reaching the output node without passing the same node twice.** (a) Probability distribution of n_{path} . The data for $n_{path} \leq 400$ are shown. (b) Scatter plot of n_{path} and the number of lethal edges n_L . The data for $n_{path} \leq 1000$ are shown. In both figures, orange indicates ES, and blue indicates random sampling. While the data for $f \in [0.99, 1.0]$ are shown for random sampling, the data for $f \in [0.99, 0.991]$ are shown for ES.

steady state was expected to differ from random sampling considering the result shown in Fig 4. To investigate the steady state, we conducted very long simulations of Evo90. We found that the fitness of all the preserved GRNs exceeded 0.9999999 at the two-millionth generation. Such extremely high values of fitness should be an artifact of the deterministic nature of GRN dynamics and should not be considered biologically relevant. We expect that noise is important for high-fitness GRNs.

Instead of introducing noise, we imposed the upper limit $f \leq 0.99$ on fitness and conducted simulations of Evo90. In the simulations, the values of fitness greater than 0.99 were regarded as 0.99. Fig 10(a) shows the distributions of the number of lethal edges n_L for GRNs of $f = 0.99$ at the generation where the fitness of all the preserved GRNs first reached 0.99. The results of ten independent runs are shown. The number distributions differed from run to run, and while some populations exhibited a small number of lethal edges, the overall tendency was that n_L was distributed broadly. Because all the preserved GRNs have the same f , the fitness-driven

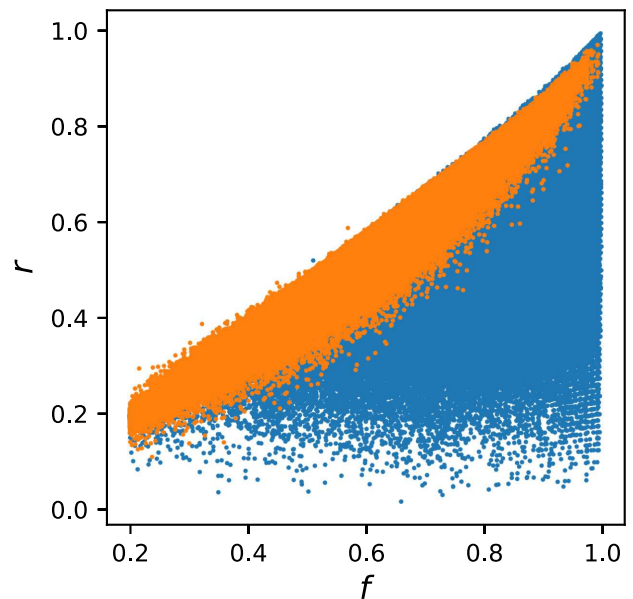


Fig 9: **Scatter plot of fitness f and robustness measure r .** The data for GRNs obtained by random sampling are presented. Each point represents a GRN. The orange points are for the monostable GRNs, and the blue points represent bistable GRNs. The strict criterion was used to determine bistability.

evolution should have ceased at the generations shown in the figure, after which the neutral evolution would continue.

We found that the distribution became steady after approximately 2000 generations. Then, we conducted runs of one million generations and collected all the GRNs every 2000 generations. Fig 10(b) shows the average distributions of n_L for GRNs with $f = 0.99$. The results of six independent runs are shown. Only two distinct distributions were observed; six runs were classified into four and two runs. We consider that populations with the same lethal edge distribution are genetically similar. These distributions are biased to low n_L compared to Fig 10(a), and the peaks of n_L are 2 and 4 for the two distributions. Moreover, the ratio of GRNs without a lethal edge reaches approximately 4% of each population. These results indicate that after the fitness distribution reached the maximum, the selection driven by the mutational robustness progressed until a steady state was reached. As a result, only a limited number of genotypic groups remained in the steady state; in these six runs, we observed that they converged to only two distinct groups.

IV. SUMMARY AND DISCUSSIONS

In this paper, we have proposed a new numerical method for studying the properties of evolutionary processes. By generating a reference set via random sampling using the multicanonical ensemble Monte Carlo

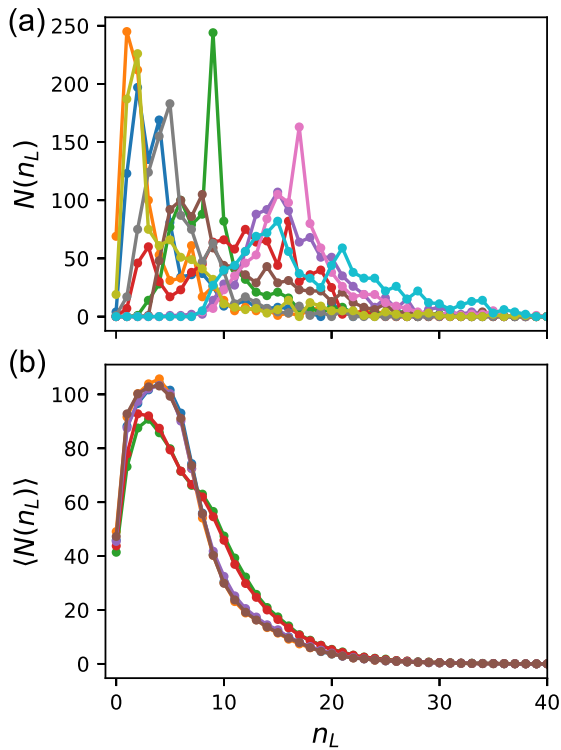


Fig 10: **Distribution of the number of lethal edges n_L for GRNs with $f = 0.99$.** We introduced the upper limit of 0.99 for fitness, and conducted Evo90. In other words, a fitness larger than 0.99 was regarded as $f = 0.99$. The data for all GRNs with $f = 0.99$ in each population were used. (a) Distribution of n_L at the generation where the fitness of all the preserved GRNs first reached 0.99. The results of ten independent runs are shown. (b) Average distribution of n_L in the steady state. After 2000 generations, we collected all the GRNs every 2000 generations up to one million generations and took their average. The results of six independent runs are shown.

method and comparing it with the outcomes of evolutionary simulations, we can quantitatively explore the universal properties and particularity of evolution. This method is both powerful and general. We investigated the evolution of a gene regulatory network model.

Random sampling revealed that almost all (probably all) GRNs become bistable as fitness approaches its maximum value. Thus, bistability is an inevitable consequence of an increase in fitness, irrespective of the evolutionary pathway. We confirmed this by using evolutionary simulations. Since bistability is not taken into account explicitly in fitness, it is an emergent property. We may regard bistability as a “new phenotype” because monostable GRNs and bistable GRNs are intrinsically different dynamical systems, and while the bistable GRNs exhibit a saddle-node bifurcation, the monostable GRNs do not. The present results indicate that the emergence of this new phenotype is a universal phenomenon that would always appear even if the evolution was re-wound and restarted. Nagata and Kikuchi obtained the

same results for their GRN model[24]. In contrast to our model, in which any network structures were allowed, they imposed restrictions on network structure; auto-regulation and mutual regulations were prohibited. As a result, the distributions of the network motifs were different for the two models. Nevertheless, both models exhibited similar bistability. Thus, bistability is a universal property for both models, irrespective of the network structure details. This observation implies that the possible phenotype is constrained by the form of the fitness function.

The response function we used is non-cooperative so that, for example, a well-known toggle-switch motif, that is, the mutual repression of two genes accompanied by auto-activations of both genes, alone does not give rise to bistability. Thus, the observed bistability is a cooperative phenomenon of many genes. The emergence of the cooperative response of GRNs consisting of many genes with non-cooperative response functions has been pointed out based on a numerical study[36]. Our results are consistent with the findings of this previous study. Another previous study found experimentally that a motif with a non-cooperative response gives rise to cooperative bistability when built in a larger GRN, although the mechanism of this cooperativity may be different from that in the present case[50]. In contrast, when the response of each gene is ultrasensitive, small motifs can exhibit bistability. The global structure of the network should differ largely in such cases; thus, we consider that the present results apply mainly to large GRNs.

By comparing the outcomes of the evolutionary simulations with random sampling, we clarified that the appearance of bistability is significantly delayed in evolution. At the same time, we found that the bistable group of GRNs contained many mutationally fragile GRNs compared to the monostable group. In other words, bistable GRNs and monostable GRNs are intrinsically different in mutational robustness. This is a nontrivial finding, which was revealed by our methodology. From this observation, we conclude that the reason for the delay in the emergence of bistability by evolution is that mutationally robust GRNs are favored in evolution. Nevertheless, as mentioned above, since almost all GRNs become bistable in the high-fitness limit, the evolutionary process should eventually produce a new phenotype, bistability. Thus, bistable and comparatively robust GRNs were selected in evolution. Whether this scenario applies to other phenotypes when different fitness functions are considered is of interest for future studies.

We found that mutational robustness was enhanced during evolution. In our model, the evolution progresses in two stages. In the early stage, the mutational robustness measure had the same values as those in the random sampling. In contrast, in the later stage, mutational robustness was markedly enhanced, as fitness increased, compared to that in the randomly sampled set of the same fitness. The mechanism for this enhancement can be explained by “second-order selection”[2]. The muta-

tion we considered consisted of two successive procedures. First, a randomly selected edge is deleted. Next, a new edge is added between a randomly selected node pair. For fitness values higher than some intermediate values, the edges start to be divided roughly into two types, as observed in Ref. [24]; neutral ones, and those causing substantially decreased fitness when deleted. Here, we name the latter type as “lethal,” although fitness does not necessarily drop close to zero unless the fitness before the deletion is large enough. If the deleted edge is lethal, fitness drops considerably, and the possibility of fitness to recover via random addition of a new edge is very low. Therefore, the more lethal edges a GRN has, the harder it is for its copy to survive.

Evolutionary enhancement of mutational robustness has been discussed for a GRN model with two-valued fitness. Ciliberti *et al.* identified GRNs with a target expression pattern as viable and investigated the effect of natural selection on the viability of mutational robustness[11]. They reported that mutational robustness is enhanced significantly in GRNs that experienced natural selection compared to that of GRNs randomly selected from viable ones. Several different selection pressures have also been reported to lead GRNs to mutationally robust ones[51]. Our results were consistent with these findings. It should be noted that we showed that the enhancement of mutational robustness was observed during the evolution of fitness. Despite the fact that selection is imposed only on fitness, selection of mutationally robust GRNs proceeds with an increase in fitness. We would like to emphasize that mutational robustness does not evolve after the evolution of fitness ceases, but they evolve simultaneously.

According to the theoretical argument based on population dynamics, when a product of the population size N and mutation rate μ is sufficiently large, mutational robustness is enhanced by neutral evolution[52]. In our case, the evolution was not neutral. However, since mutations that increase fitness are rare, almost all mutations are either deleterious or almost neutral. Thus, evolution is in most part neutral. The deleterious mutations are deleted by selection. In contrast, mutationally robust GRNs are favored in the case of almost neutral mutations. Therefore, while fitness increases intermittently, robustness continues to increase during the period of neutral evolution. In the case of GRNs, the above condition is modified to $PN\mu \gg 1$, where μ is the mutation rate per gene[2]. Because μ is comparatively large in our ES, this condition is considered to be satisfied, and second-order selection works. In this scenario, mutational robustness is enhanced because GRNs containing many lethal edges are easily eliminated from the population. While the above population dynamical theory is for the steady state of evolution, our result was for the transient process of evolution as mentioned above. Thus, the argument above is more or less speculative.

A set of GRNs with high fitness, such as $f \geq 0.99$, compose the neutral space. Thus, we collected the members

of the neutral space using our method of random sampling by McMC. Ciliberti *et al.* analyzed the structure of the neutral space for the above-mentioned model in which simple random sampling was valid and found that the high-fitness GRNs belong to a large neutral space[11]. Unfortunately, a similar analysis was difficult for GRNs obtained using McMC. Instead, we set the maximum value $f = 0.99$ and regarded all fitness values greater than it as 0.99 for conducting long ES. After all preserved GRNs reached this maximum value, the neutral evolution continued, and eventually, the steady state was reached. Based on the lethal edge distribution, we conclude that mutational robustness increased during neutral evolution. We found that the populations converged to a small number of distinct distributions of lethal edges. In the present study, the six runs converged to only two distributions. It is natural to assume that GRNs with the same lethal edge distribution belong to the same neutral space or the same attractor in the neutral space. Thus, we consider that the neutral space is divided into only a small number of parts. This finding is consistent with that reported in Ref. [11]. The situation is similar to that studied by population dynamics mentioned above and is consistent with it given $PN\mu \gg 1$ [52]. The population dynamical theory showed that the topology of the neutral space was the main factor in determining mutational robustness. We would like to conduct a detailed analysis of the neutral space for future research.

Next, we discuss network motifs. Some characteristic motifs were found for highly fit GRNs, although these were not prominent compared to those for the model in Ref [24]. This difference is attributed to the differences in the allowed network structures. Among these motifs, coherent feedforward loops are frequently observed in real GRNs[27, 49, 53]. The following structures are also identified as motifs, which are known to exhibit bistability if the response of each gene is ultrasensitive[26, 35, 54–59]: auto-activation, mutual-activation, mutual-repression, and mutual-activation/repression accompanied by auto-activations of both genes. The last motif is widely observed in multistable GRNs[14, 28, 29, 60–62]. As mentioned above, bistability was not realized by these single motifs but realized as a cooperative phenomenon of many genes. Nevertheless, these motifs were observed in our model, although they were not indispensable. However, they are not relevant to the mutational robustness. This implies that mutational robustness is related to the global structure of GRNs. We found that the number of paths connecting the input and output nodes differed between randomly sampled GRNs and evolutionarily obtained ones. Although it is understandable that GRNs having many such paths are robust because of redundancy, this does not fully explain the origin of mutational robustness.

Evolutionary speed is roughly determined by the number of available GRNs or, in other words, “genotypic entropy.” This is a consequence of our definition of a single-valued fitness function, which can be computed from the

dynamics of a given GRN for a predetermined single task and has the maximum value. This setup is somewhat artificial, and fitness is not a simple function in reality. However, some experimental studies have addressed the situation discussed in this study. For example, Sato *et al.* reported such an evolutionary study, although they did not deal with a GRN but a protein[63]. They put DNA encoding the green fluorescent protein along with a random sequence into the genome of *E. coli* and conducted artificial evolution with selection based on fluorescence intensity. In this experiment, an observable single-valued fitness was set, which had the maximum value. They found that the evolutionary speed decreased as fluorescence intensity increased. We consider that the variation in evolutionary speed in their experiment is explained almost fully by the entropic effect. In a natural situation departing from the experimental condition, evolution is not restricted to proceeding in only one direction. When evolution in one direction becomes difficult, the direction changes. We consider that the concept of the genotypic entropy effect on evolutionary speed can also apply to such a natural situation.

We believe that the three main results, that is, the evolution of mutational robustness, delay in the emergence of a new phenotype, and relationship between evolutionary speed and genetic entropy, apply generally to living systems, because they are naturally understandable. Similar studies using different models and other objects are necessary to confirm this hypothesis.

V. METHODS

A. Random sampling

Random sampling was realized by the MCMC method (more precisely, entropic sampling[64], which is one of the variations of MCMC). Details of this method are described in Ref. [24]. We divided the fitness into 100 bins and determined the weight for each bin so that the GRNs appeared evenly, using the Wang-Landau method[65, 66]. One MCMC update consisted of the following two successive processes: deleting a randomly selected edge and adding a new edge to an unlinked node pair that was also chosen randomly. Whether to accept this change was determined using the Metropolis method. One Monte Carlo step (MCS) consisted of K such updates, and we recorded f at every MCS. We sampled GRNs every 20 MCSs to reduce the correlation between the samples. We conducted ten independent runs, each consisting of 10^7 MCSs. As

a result, we obtained an average of 50,000 samples for each bin. Ideally, we gathered GRNs randomly within each bin; although inter-sample correlations should have remained to some extent, we named this method “random sampling” in this study. The set of these randomly sampled GRNs was considered as the reference set.

B. Evolutionary simulation

We conducted two types of evolutionary simulations: Evo50 and Evo90. For both simulations, we prepared an initial population consisting of 1000 randomly generated GRNs. The population size remained unchanged during the simulations. In each generation of Evo50, we selected the top 500 GRNs according to the level of fitness and made one copy for each. In the case of Evo90, 90% of the population, namely, 900 GRNs, from the highest fitness is selected for preservation, and the remaining 10% of GRNs were discarded in each generation. We randomly selected 100 GRNs from the preserved 900 GRNs and made one copy for each. Then, these copies were subjected to mutation for both simulations. The mutation procedure for each GRN was the same as in the MCMC procedure; an edge was deleted randomly from the network, and a new edge was then added between a randomly selected unlinked node pair. As these procedures were repeated, the average fitness of the population increased. After 150 generations for Evo50 and 200 generations for Evo90, we picked the GRN with the highest fitness in the population and traced its ancestors to obtain a single lineage. The population size and number of generations were determined arbitrarily. We repeated this evolutionary simulation 100,000 times and 55,000 times independently for Evo50 and Evo90, respectively, and, as a result, we collected 100,000 lineages and 55,000 lineages, respectively.

C. Data availability

Source codes and data are available at Zenodo repository (DOI:10.5281/zenodo.4409496).

Acknowledgments

We thank Koich Fujimoto, Masayo Inoue, Katsuyoshi Matsushita, Nobu C. Shirai, and Hajime Yoshino for their fruitful discussions and comments. We also thank Editage for English language editing.

[1] Kitano H. Biological robustness. *Nat Rev Genet.* 2004;5:828–837.

[2] Wagner A. *Robustness and Evolvability in Living Systems.* Princeton Univ Press; 2005.

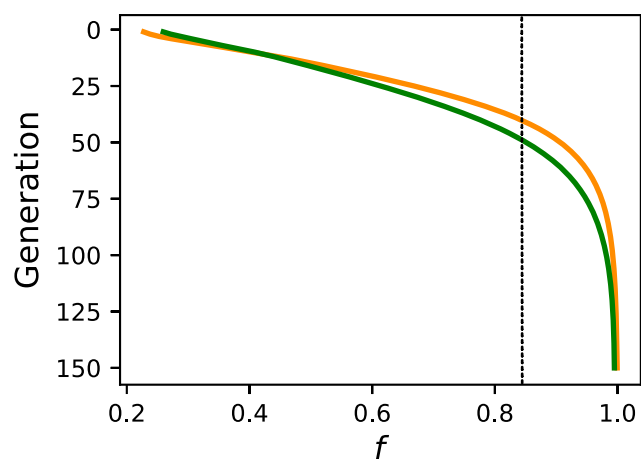
[3] Masel J, Siegal ML. Robustness: mechanisms and consequences. *Trends Genet.* 2009;25:395–403.

[4] Giaever G, Chu AM, Ni L, Connelly C, Riles L, Veroneau S, et al. Functional profiling of the *Saccharomyces*

- cerevisiae* genome. *Nature*. 2002;418:387–391.
- [5] Baba T, Ara T, Hasegawa M, Takai Y, Okumura Y, Baba M, et al. Construction of *Escherichia coli* K-12 in-frame, single-gene knockout mutants: the Keio collection. *Mol Syst Biol*. 2006;2:2006.0008.
- [6] Kim DU, Hayles J, Kim D, Wood V, Park HO, Won M, et al. Analysis of a genome-wide set of gene deletions in the fission yeast *Schizosaccharomyces pombe*. *Nat Biotechnol*. 2010;28:617–623.
- [7] Isaran M, Lemerle C, Michalodimitrakis K, Horn C, Beltrao P, Raineri E, et al. Evolvability and hierarchy in rewired bacterial gene networks. *Nature*. 2008;452:840–845.
- [8] Kauffman SA. Metabolic stability and epigenesis in randomly constructed genetic nets. *J Theor Biol*. 1969;22:437–467.
- [9] Kauffman SA, Levin S. Towards a general theory of adaptive walks on rugged landscapes. *J Theor Biol*. 1987;128:11–45.
- [10] Kauffman SA. *The Origins of Order: Self-Organization and Selection in Evolution*. Oxford Univ Press; 1993.
- [11] Ciliberti S, Martin OC, Wagner A. Robustness can evolve gradually in complex regulatory gene networks with varying topology. *PLoS Comput Biol*. 2007;3:e15.
- [12] Ciliberti S, Martin OC, Wagner A. Innovation and robustness in complex regulatory gene networks. *Proc Natl Acad Sci USA*. 2007;104:13591–13596.
- [13] Schuster P, Fontana W, Stadler PF, Hofacker IL. From sequences to shapes and back: a case study in RNA secondary structures. *Proc R Soc Lond B*. 1994;255:279–284.
- [14] Burda Z, Krzywicki A, Martin OC, Zagorski M. Motifs emerge from function in model gene regulatory networks. *Proc Natl Acad Sci USA*. 2011;108:17263–17268.
- [15] Zagorski M, Krzywicki A, Martin OC. Edge usage, motifs, and regulatory logic for cell cycling genetic networks. *Phys Rev E*. 2013;87:012727.
- [16] Saito N, Kikuchi M. Robustness leads close to the edge of chaos in coupled map networks: toward the understanding of biological networks. *New J Phys*. 2013;15:053037.
- [17] Berg BA, Neuhaus T. Multicanonical algorithms for first order phase transitions. *Phys Lett*. 1991;B267:249–253.
- [18] Berg BA, Neuhaus T. Multicanonical ensemble: A new approach to simulate first-order phase transitions. *Phys Rev Lett*. 1992;68:9–12.
- [19] Saito N, Iba Y, Hukushima K. Multicanonical sampling of rare events in random matrices. *Phys Rev E*. 2010;82:031142.
- [20] Saito N, Iba Y. Probability of graphs with large spectral gap by multicanonical Monte Carlo. *Comput Phys Commun*. 2011;182:223–225.
- [21] Kitajima A, Iba Y. Multicanonical sampling of rare trajectories in chaotic dynamical systems. *Comput Phys Commun*. 2011;182:251–253.
- [22] Iba Y, Saito N, Kitajima A. Multicanonical MCMC for sampling rare events: an illustrative review. *Ann Inst Stat Math*. 2014;66:611.
- [23] Kitajima A, Kikuchi M. Numerous but rare: An exploration of magic squares. *PLoS ONE*. 2015;10:e0125062.
- [24] Nagata S, Kikuchi M. Emergence of cooperative bistability and robustness of gene regulatory networks. *PLoS Comput Biol*. 2020;16:e1007969.
- [25] Goldbeter A, Koshland DE. An amplified sensitivity arising from covalent modification in biological systems. *Proc Natl Acad Sci USA*. 1981;78:6840–6844.
- [26] Ferrell JE, Ha SH. Ultrasensitivity part I: Michaelian responses and zero-order ultrasensitivity. *Trends Biochem Sci*. 2014;39:496–503.
- [27] Alon U. *An Introduction to Systems Biology* (second edition). CRC Press; 2020.
- [28] Ptashne M, Gann A. *Genes & Signals*. Cold Spring Harbor Laboratory Press; 2002.
- [29] Ptashne M. *A Genetic Switch* (third edition). Cold Spring Harbor Laboratory Press; 2004.
- [30] Zong C, h So L, Sepuveda LA, Skinner SO, Golding I. Lysogen stability is determined by the frequency of activity bursts from the fate-determining gene. *Mol Syst Biol*. 2010;6:440.
- [31] Watson JD, Baker TA, Bell SP, Gann A, Levine M, Losick R. *Molecular Biology of the Gene* (7th edition). Pearson Education; 2013.
- [32] Pomerening JR, Sontag ED, Ferrell JE. Building a cell cycle oscillator: hysteresis and bistability in the activation of Cdc2. *Nat Cell Biol*. 2003;5:346–351.
- [33] Sha W, Moore J, Chen K, Lassaletta AD, Yi CS, Tyson JJ, et al. Hysteresis drives cell-cycle transitions in *Xenopus laevis* egg extracts. *Proc Natl Acad Sci USA*. 2003;100:975–980.
- [34] Trunnell NB, Poon AC, Kim SY, Ferrell JE. Ultrasensitivity in the regulation of Cdc25C by Cdk1. *Mol Cell*. 2011;41:263–274.
- [35] Ferrell JE, Machleder EM. The biochemical bases of an all-or-none cell fate switch in *Xenopus* oocytes. *Science*. 1998;280:895–898.
- [36] Inoue M, Kaneko K. Cooperative reliable response from sloppy gene-expression dynamics. *Eutophys Lett*. 2018;124:38002.
- [37] Mjolsness E, Sharp DH, Reinitz J. A connectionist model of development. *J Theor Biol*. 1991;152:429–453.
- [38] Wagner A. Evolution of gene networks by gene duplications: A mathematical model and its implications on genome organization. *Proc Natl Acad Sci USA*. 1994;91:4387–4391.
- [39] Wagner A. Does evolutionary plasticity evolve. *Evolution*. 1996;50:1008–1023.
- [40] Siegal ML, Bergman A. Waddington’s canalization revisited: developmental stability and evolution. *Proc Natl Acad Sci USA*. 2002;99:10528–10532.
- [41] Masel J. Genetic assimilation can occur in the absence of selection for the assimilating phenotype, suggesting a role for the canalization heuristic. *J Evol Biol*. 2004;17:1106–1110.
- [42] Kaneko K. Evolution of robustness to noise and mutation in gene expression dynamics. *PLoS one*. 2007;2:e434.
- [43] Espinosa-Soto C, Martin OC, Wagner A. Phenotypic robustness can increase phenotypic variability after non-genetic perturbations in gene regulatory circuits. *J Evol Biol*. 2011;24:1284–1297.
- [44] Inoue M, Kaneko K. Cooperative adaptive responses in gene regulatory networks with many degrees of freedom. *PLoS Comput Biol*. 2013;9:e1003001.
- [45] Furusawa C, Kaneko K. A generic mechanism for adaptive growth rate regulation. *PLoS Comput Biol*. 2008;4:e3.
- [46] Pujato M, MacCarthy T, Fiser A, Bergman A. The underlying molecular and network level mechanisms in the evolution of robustness in gene regulatory networks. *PLoS Comput Biol*. 2013;9:e1002865.

- [47] Hopfield JJ, Tank DW. “Neural” Computation of Decisions in Optimization Problems. *Biol Cybern.* 1985;52:141–152.
- [48] Tyson JJ, Chen KC, Novak B. Sniffers, buzzers, toggles and blinkers: dynamics of regulatory and signaling pathways in the cell. *Curr Opin Cell Biol.* 2003;15:221–231.
- [49] Shen-Orr SS, Milo R, Mangan S, Alon U. Network motifs in the transcriptional regulation network of *Escherichia coli*. *Nat Genet.* 2002;31:64–68.
- [50] Tan C, Marguet P, You L. Emergent bistability by a growth-modulating positive feedback circuit. *Nat Chem Biol.* 2009;5:842–848.
- [51] Espinosa-Soto E. Selection for distinct gene expression properties favours the evolution of mutational robustness in gene regulatory networks. *J Evol Biol.* 2016;29:2321–2333.
- [52] van Nimwegen E, Crutchfield JP, Huynen M. Neutral evolution of mutational robustness. *Proc Natl Acad Sci USA.* 1999;17:9716–9720.
- [53] Mangan S, Alon U. Structure and function of the feed-forward loop network motif. *Proc Natl Acad Sci USA.* 2003;100:11980–11985.
- [54] Ferrell JE, Xiong W. Bistability in cell signaling: How to make continuous processes discontinuous, and reversible processes irreversible. *Chaos.* 2001;11:227–236.
- [55] Ferrell JE. Self-perpetuating states in signal transduction: positive feedback, double-negative feedback and bistability. *Curr Opin Chem Biol.* 2002;6:140–148.
- [56] Angeli D, Ferrell JE, Sontag ED. Detection of multistability, bifurcations, and hysteresis in a large class of biological positive-feedback systems. *Proc Natl Acad Sci USA.* 2003;101:1822–1827.
- [57] Pfeuty B, Kaneko K. The combination of positive and negative feedback loops confers flexibility to biochemical switches. *Phys Biol.* 2009;6:046013.
- [58] Tiwari A, Igoshin OA. Coupling between feedback loops in autoregulatory networks affects bistability range, open-loop gain and switching times. *Phys Biol.* 2012;9:055003.
- [59] Ferrell JE, Ha SH. Ultrasensitivity part III: cascades, bistable switches, and oscillators. *Trends Biochem Sci.* 2014;39:612–618.
- [60] Huang S, Guo YP, May G, Enver T. Bifurcation dynamics in lineage-commitment in bipotent progenitor cells. *Dev Biol.* 2007;305:695–713.
- [61] Jia D, Jolly MK, Harrison W, Boaretto M, Ben-Jacob E, Levine H. Operating principles of tristable circuits regulating cellular differentiation. *Phys Biol.* 2017;14:035007.
- [62] Huang B, Lu M, Jia D, Ben-Jacob E, Levine H, Onuchic JN. Interrogating the topological robustness of gene regulatory circuits by randomization. *PLoS Comput Biol.* 2017;13:e1005456.
- [63] Sato K, Ito Y, Yomo T, Kaneko K. On the relation between fluctuation and response in biological systems. *Proc Natl Acad Sci USA.* 2003;100:14086–14090.
- [64] Lee J. New Monte Carlo Algorithm: Entropic Sampling. *Phys Rev Lett.* 1993;71:211–214.
- [65] Wang F, Landau DP. Efficient, Multiple-Range Random Walk Algorithm to Calculate the Density of State. *Phys Rev Lett.* 2001;86:2050—2053.
- [66] Wang F, Landau DP. Determining the density of states for classical statistical models: A random walk algorithm to produce a flat histogram. *Phys Rev E.* 2001;64:056101.

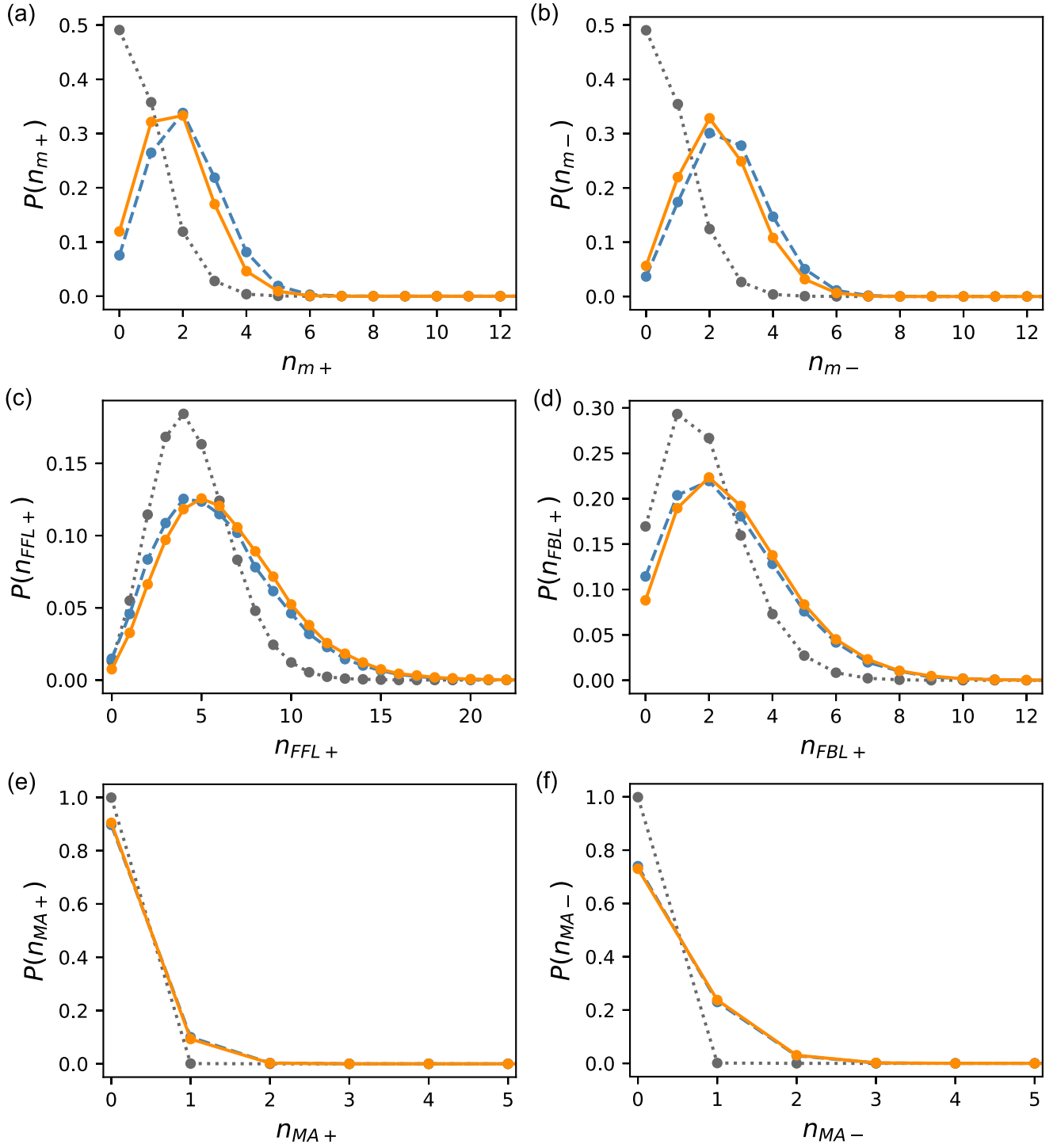
Supporting information



S1 Fig. Evolution of fitness for Evo50 and Evo90.

The orange and green lines represent the average fitness of each generation calculated for lineages obtained by evolutionary simulations, Evo50 and Evo90, respectively.

Averages were taken over 100,000 and 55,000 lineages, respectively. The vertical line indicates the fitness at which $\Omega(f)$ starts to decrease faster than the exponential rate.



S2 Fig. Probability distributions of the number of motifs. The data for $f \in [0.99, 1.0]$ are shown. The orange solid lines represent Evo50, and the blue dashed lines represent random sampling. The distributions for the random networks are also shown as references with the gray dotted lines. The distributions for the evolutionary simulation were corrected using the reweighting method described in the text. (a) Mutual-activation (b) Mutual-repression (c) Coherent feed-forward loop (d) Positive feedback loop (e) Mutual-activation accompanied by auto-activations of both genes (f) Mutual-repression accompanied by auto-activations of both genes.